Homology modeling, molecular docking and electrostatic potential analysis of MurF ligase from *Klebsiella pneumonia*

Venkatabalasubramanian Sivaramakrishnan[1], Chinnaiyan Thiyagarajan[2], Sivakumaran Kalaivanan[2], Raj Selvakumar[2], Muthuswamy Anusuyadevi[3] & Kesavan Swaminathan Jayachandran[2]*

[1]Department of Bioinformatics, School of chemistry and biotechnology, SASTRA University, Thirumalaisamudram, Thanjavur-613402, Tamilnadu, India; [2]Department of Bioinformatics, Bharathidasan University, Palkalaiperur, Tiruchirapalli-620024, Tamilnadu, India; [3]Department of Biochemistry, Bharathidasan University, Palkalaiperur, Tiruchirapalli-620024, Tamilnadu, India; Kesavan Swaminathan Jayachandran – E-mail: s.jayachandran@bdu.ac.in, Phone: +91-8344146040; *Corresponding author

Abstract:
In spite of availability of moderately protective vaccine and antibiotics, new antibacterial agents are urgently needed to decrease the global incidence of *Klebsiella pneumonia* infections. MurF ligase, a key enzyme, which participates in the bacterial cell wall assembly, is indispensable to existence of *K. pneumonia*. MurF ligase lack mammalian vis-à-vis and have high specificity, uniqueness, and occurrence only in eubacteria, epitomizing them as promising therapeutic targets for intervention. In this study, we present a unified approach involving homology modeling and molecular docking studies on MurF ligase enzyme. As part of this study, a homology model of *K. pneumonia* (MurF ligase) enzyme was predicted for the first time in order to carry out structure-based drug design. The accuracy of the model was further validated using different computational approaches. The comparative molecular docking study on this enzyme was undertaken using different phyto-ligands from *Desmodium sp.* and a known antibiotic Ciprofloxacin. The docking analysis indicated the importance of hotspots (HIS 281 and ASN 282) within the MurF binding pocket. The Lipinski's rule of five was analyzed for all ligands considered for this study by calculating the ADME/Tox, drug likeliness using Qikprop simulation. Only ten ligands were found to comply with the Lipinski rule of five. Based on the molecular docking results and Lipinki values 6-Methyltetrapterol A was confirmed as a promising lead compound. The present study should therefore play a guiding role in the experimental design and development of 6-Methyltetrapterol A as a bactericidal agent.

Background:
Klebsiella pneumonia (KN) belonging to the *enterobacteriaceae* family is a gram-negative, rod-shaped, non-motile, encapsulated bacterial pathogen. Its continued global challenge has precipitated the emergence of pandrug-resistant clones to clinically pertinent antibiotics (e.g. Fluroquinones, third-generation cephalosporins and carbapenems) that resulted in limited therapeutic strategies to combat this pathogen [1-3]. Hence, the compelling need to develop novel and potent anti-bacterial drugs to overcome this pathogen is of global concern and national importance. Most of the antibiotics designed by the researchers over last five decades have focused on either improving the design or structure of an agent that could intervene with the peptidoglycan biosynthesis process or inhibit a key enzyme involved in its assembly [4]. Peptidoglycan layer is considered to be indispensable to bacterial cell wall providing it structural integrity and protection against osmotic pressure. The peptidoglycan biochemical assembly involves both

extracellular and intracellular pathways **[4].** Among them only the extracellular pathway has been extensively studied and over-exploited for anti-bacterial intervention. The intracellular stage of peptidoglycan biosynthesis involving the ATP-dependent Mur ligases (MurC, MurD, MurE and MurF) have been least studied **[4].** Hence to explore this (MurF) pathway of KN as an option for bactericidal drug development the present study was undertaken.

MurF catalyzes the last cytoplasmic step of ligation of D-Ala-DAla to UDP-MurNAc-tripeptide (UDP-MurNAc-L-Ala-γ-D-Glu-meso-diaminopimelate), with hydrolysis of ATP resulting in synthesis of UDP-MurNAc-pentapeptide **[4].** MurF lacks human counterparts and are unique and highly conserved among various bacterial species rendering them as promising therapeutic targets for intervention. Due to the above mentioned reason, a potential MurF inhibitor would be expected to be bactericidal and to have a wide spectrum action against gram negative pathogens, which validates its choice as a target for the development of new inhibitors/bactericidals **[5].** The search for new biologically active compounds from natural sources is currently of great interest as they are the parent compounds for most of presently available commercial bactericidal agents/inhibitors/antibiotics. Numerous *in vitro* (10 µM < IC 50 > 20 µM) reports suggest the aqueous, alcoholic and acetone extracts of *Desmodium* plant sp. possesses potential bactericidal activity against *enterobacteriaceae* family of pathogens. *Desmodium* flora species have a long history of being used in Indian ayurvedic medicine and Chinese traditional medicine against such *enterobacteriaceae* pathogens **[6].** Here, we chose few recently reported phyto-ligands from this plant for our structure based drug designing (SBDD) study, viz., 6-Methyltetrapterol A (6MT), Uncinanone A, Uncinanone B, Uncinanone C, Uncinanone D, Uncinanone E, Quercetin, Hydnocarpin, Edudiol, Hydroxydesmodian B, Desmodol, Desmodian C, Desmodian D and Yukovanol **[6].**

Virtual screening has become increasingly popular in hit discovery and lead compound optimization. Comparisons based on Lipinski analysis for all phyto-ligands were pursued to suggest the drug likeliness of active principles/phytoligands of *Desmodium* plant sp considered for this study. The results of *in silico* interactions studies of MurF with all the above mentioned phyto-ligands were compared with interactions of Ciprofloxacin (CP - Fluroquinone drug used as last resort broad spectrum anti-bacterial agent) to show the bactericidal potency of the phyto-ligands. The primary objective of the present work is to report the three-dimensional model of KN-MurF enzyme for the first time. KN-MurF provides the geometry of hot spot regions, i.e., binding site residues, and therefore provides a clear insight into the importance of the active site residues in terms of their contribution to protein-ligand complexes. Moreover, the rational design of an inhibitor selective towards the KN-MurF enzyme could be more effective if the key residues and atomic level binding site interactions are known. A unified approach involving homology modeling, molecular docking and electrostatic potential analysis was applied to KN-MurF to probe its active site residues, interactions, thereby revealing its mechanism of action.

Methodology:
All computations and SBDD of KN-MurF enzyme were carried out on a Pentium IV Dual Core processor workstation with Windows 7 operating system using Accelrys Draw (v4.0), Autodock (v4.2), Schrödinger (v9.2), Swiss-PdbViewer (v4.04) and Chimera (v1.5.3) molecular modeling packages **[7-10].**

Sequence analysis and physiochemical characterization
KN-MurF Ligase protein sequence (ID: A6T4M9) was retrieved from Uniprot database in FASTA format. Its physiochemical characterization was computed using the Expasy Protparam program. Secondary structure prediction analysis was performed using SABLE program **[11].** Template (*Escherichia coli*-MurF: 1GG4_A) was selected by performing BLAST search against protein databank (PDB) with > 80% sequence identity cut off for homology modeling. Alignment between target KN sequence (KN-MurF Ligase) and the template *Escherichia coli* (EC) sequence (EC-MurF Ligase, PDB ID: 1GG4_A) was performed with Multalin tool and visualized using ES pript **[12, 13].**

Homology modeling and validation
Tertiary structure prediction was performed using I-Tasser Server for homology modeling **[14].** The plausible models of KN-MurF obtained from I-Tasser server were verified by Structural Analysis and Verification Server (SAVES) to evaluate its stereo-chemical quality **[15, 16].**

Ligand preparation and ADME/Tox Prediction
The structures of 14 phyto-ligands and 1 antibiotic, Ciprofloxacin, were sketched with Accelrys Draw (v4.0). Each structure was launched in ligprep (Schrödinger) and energy minimized using the OPLS force field and geometrically optimized followed by Lipinski's values/ADME-Tox prediction by using Qikprop (Schrödinger).

Molecular Docking
Docking analysis of KN-MurF1 was carried out using Autodock (v4.2) with the aim of exposing the active site amino acid residues involving protein-ligand interactions so as to obtain information about the bioactive conformation of these KN-MurF inhibitors. From the ADT package hydrogen atoms were added, Nonpolar hydrogens and lone pairs were merged and each atom within the macromolecule was assigned a Gasteiger partial charge. A grid box of 80×80×80, with a spacing of 0.447 Å was positioned using autogrid and blind docking was performed. The Lamarckian genetic algorithm (LGA) of up to 20 runs was employed with the settings of population size of 150 individuals, maximum number of generations and energy evaluations of 27,000 and 2.5 million respectively. From the estimated free energy of ligand binding (ΔG), the inhibition constant (Ki) for each ligand was calculated. K_i is calculated by the equation: $K_i = \exp[(\Delta G^* 1000)/(R^*T)]$ Where ΔG is docking energy, R (gas constant) is 1.98719 cal K^{-1} mol^{-1} and T (Temperature) is 298.15 K. Only the best pose (the one with the lowest binding energy) was considered for each ligand. All previously mentioned phyto-ligands after ligand preparation were docked successfully in the active site of the model KN-MurF1 enzyme. Molecular visualization of the docked complexes was carried out with Chimera (v1.5.3).

Molecular electrostatic potential analysis
The Molecular electrostatic potential (MEP) analysis at the functional binding pocket of KN-MurF1-6-MT complex and KN-MurF1-CP complex were carried out using Swiss-PdbViewer (v4.04) to visually compare two molecules with its

ligands based on their surface level potential values. To both structures Poisson-Boltzmann based molecular surface was generated and visualized independently.
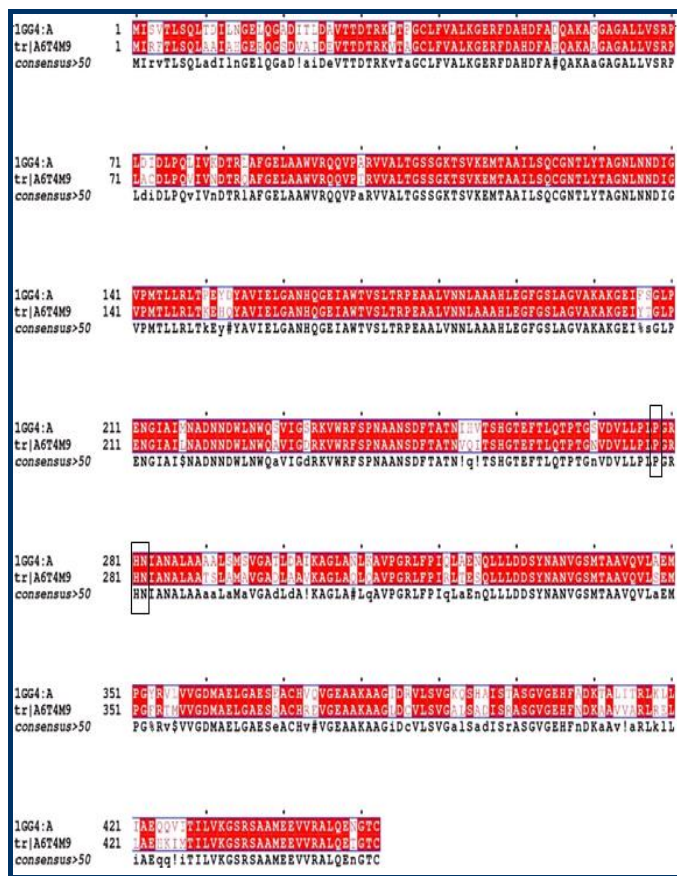

Figure 1: The alignment between target and template sequence

Discussion:

The physiochemical characterization of KN-MurF protein revealed the following: Sequence length (452 amino acid residues); Molecular weight (47.5 KDa); Theoretical Iso-electric point (5.53); Major residues (Ala 15.7% and Leu 10.8%); Total number of negatively charged residues (Asp + Glu): 46; Total number of positively charged residues (Arg + Lys): 36; Extinction coefficient (33835 M^{-1} cm^{-1}); Instability index (25.81); Aliphatic index (98.54) and Grand average of hydropathicity (GRAVY): 0.118.

Secondary analysis of KN-MurF revealed presence of 42.92% α-helix (H), 19.9% β-sheets (E) and 28% random coils (C). In the absence of experimental data, structure-building on the basis of known 3D structure (template) of a homologous protein is the only plausible method to obtain structural information which is based on sequential information [17]. The blastp results of KN-MurF revealed the availability of crystal structure of MurF (1GG4_A: Resolution 2.3 Å) from closely homologous bacterium *E. Coli* (EC) [18]. Hence, EC-MurF (PDB ID: 1GG4_A) was chosen as template to predict target KN-MurF (A6T4M9) structure due to global sequence similarity of 80% between two sequences, higher coverage >90% of aligned sequence, with least E-value (0) and higher score (721) than other PDB hits.

Since, the quality of the 3D structure of a modeled protein strongly depends on the accuracy of the template structure chosen; multiple sequence alignment (MSA) was undertaken.

MSA between target (KN-MurF: A6T4M9) and template (EC-MurF: 1GG4_A) sequence was performed to identify the sequence-structure relationship **(Figure 1)** It was found that approximately > 80% of the amino acid residues are highly conserved between them including the active site region containing residues PRO278, HIS281 and ASN282 (shown as marked boxes).
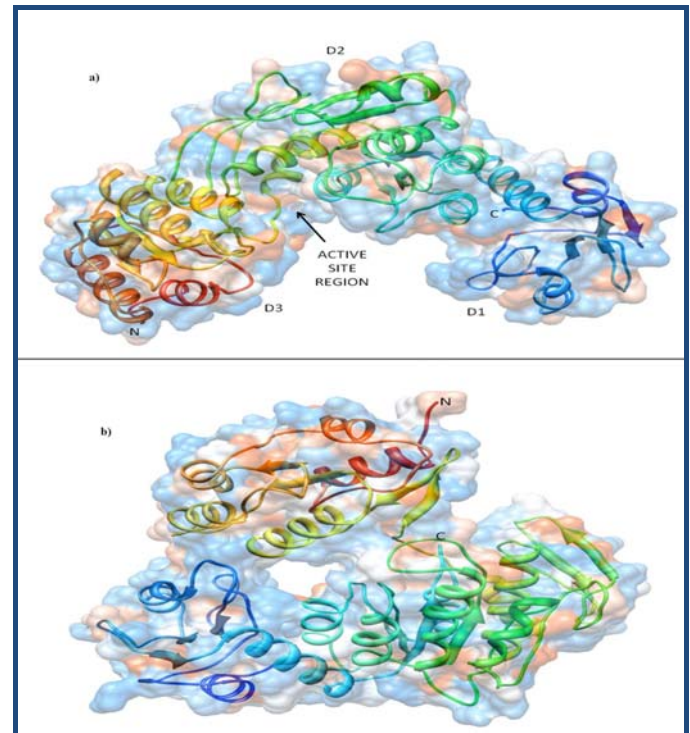

Figure 2: Target models of *K. pneumonia* (MurF Ligase): KN-MurF1 **(2a)** and KN-MurF2 **(2b)** illustrated as ribbon structure with RGB (red, green and blue) colours along with its shadow as hydrophobic surface. (D1-D3) represents three consecutive open alpha/beta-sheet domains. C and N represent C-Terminal and N-Terminal respectively

I-Tasser a web based structure prediction program was used in this study for performing template (EC-MurF) based homology modelling approach of target (KN-MurF). I-Tasser generated two plausible models KN-MurF1 and KN-MurF2 **(Figure 2a & 2b)**. Three criteria (C-Score, TM score and RMSD values) were employed to compare the quality of predicted models to choose the best one. KN-MurF1 homology model was predicted to have a C-Score 1.21 which was comparatively better than KN-MurF2 homology model C-Score of 0.22. The estimated computational TM score (0.94±0.05) and RMSD (3.8±0.2A°) of KN-MurF1 too was found to be better than the values obtained for KN-MurF2 model. KN-MurF1 expeditiously qualified all the three criteria signifying its quality as the best model.

Ramachandran plot computed by PROCHECK module of SAVES showed that only 0.3% of residues existed in disallowed regions confirming the quality of KN-MurF1 predicted to be highly significant **(Figure 3a)**. ERRAT analysis showed the overall structural quality of the predicted structure as 95.64, which is very good experimentally and computationally **(Figure 3b).** VERIFY_3D analysis showed that 98.44% of KN-MurF1 protein residues had an average 3D-1D score > 0.2 showing good primary sequence to tertiary structure compatibility.

Evaluation of KN-MurF1 structural quality with ProSA-web reveals that its ProSA Z-score value −9.22 falls in the range of native conformations computed using X-ray crystallography method represented as encircled large black dot **(Figure 3c).** The results reveal that most of the residues fall in the negative energy minima region representing good structural quality and low energy levels of the predicted protein KN-MurF1 **(Figure 3d).** Thus the various approaches elaborate the highly dependable quality and stability of predicted KN-MurF1 3D structure.
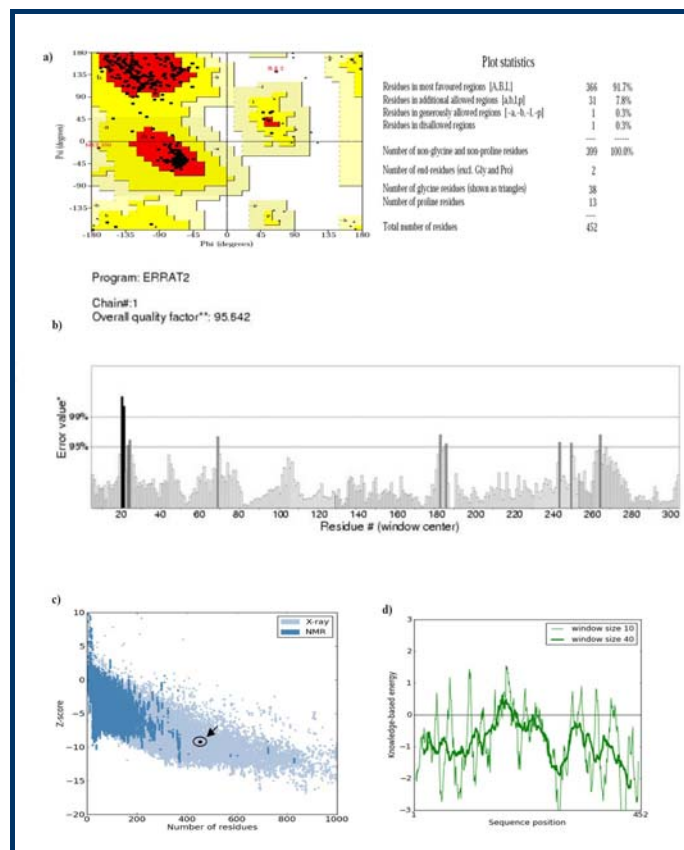
Figure 3: Stereo-chemical validation of the predicted KP-MurF1 is shown below using Ramachandran plot and its statistics from Procheck **(3a)**, ERRAT plot **(3b)**, ProSA Z-score **(3c)** and corresponding energy schema **(3d).**

ADME-Tox/Lipinski's rule of five (molecular weight < 500 Da, HB donor < 5, HB acceptor < 10 and QPlogPo/w (octanol/water partition coefficient) should be < 5) for all 14 phyto-ligands and Ciprofloxacin (CP) were generated **Table 2 (see supplementary material).** Out of the 14 phyto-ligands Hydnocarpin, Uncinanone A, Uncinanone B, Hydroxydesmodian B and Desmodian D failed to obey the Lipinski's rule of five since the number of acceptor HB were greater than 10. All the other phyto-ligands including CP comply with the Lipinski's rule of five. Hence only the rest ten ligands inclusive of ciprofloxacin were further considered for docking studies **Table 1 (see supplementary material).** The docking analysis revealed the presence of GLU116, PRO278, HIS281, ASN 282, GLN 311, VAL313, ARG316, LEU317 and SER339 residues within the vicinity of 4Å of active site of KN-MurF1. The docking results further confirmed 6-Methyltetrapterol A (6MT) as the best lead molecule due to its least docking energy, lowest Ki value and involves 3 hydrogen

bond (HB) interactions with hotspot residues PRO278, HIS281 and ASN282 of KN-MurF1 active site as compared to other ligands **Figure 4 & Table 2 (see supplementary material).**
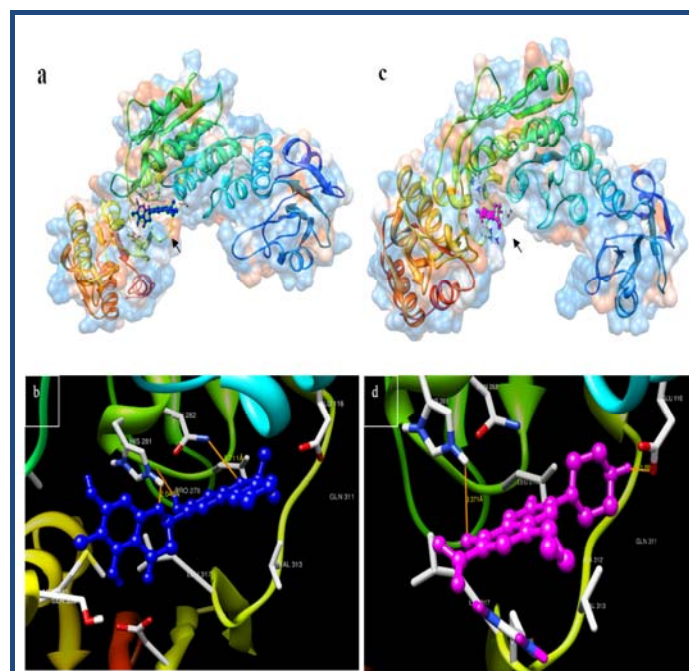

Figure 4: KN-MurF1-6-MT complex **(4a)** and KN-MurF1-CP complex **(4c)** with their corresponding interaction residues within 4Å vicinity of active site hotspots **(4b & 4d)**. 6MT- Blue colour and CP- Pink colour represented as a ball and stick model.

The docking interaction complex KN-MurF1-6MT was compared with KN-MurF1-CP (3a-3d). The active site interaction was magnified to understand the molecular conformations of ligands (CP and 6MT) docking with receptor KN-MurF1 and to gain knowledge on the ligand-receptor HB interaction (light brown colour) within the vicinity of 4 Å of active site hot spot region **(Figure 4b & 4d)**. KN-MurF1-6MT complex involves three HB interactions at PRO278, HIS281 and ASN 282 residues with a better ΔG score and least K_i Value as compared to two hydrogen bond interactions at GLU116 and HIS 281 and higher ΔG score and K_i Value of KN-MurF1-CP complex. Almost 90 degree conformational orientation of the two primary rings of ligand 6MT as compared to CP expanded KN-MurF1 active site resulting in accessing the ASN282 residue for HB interaction. The smaller ring structure of CP resulted in only partially accessing the active site resulting in the prevention of access to ASN282 as evident from the molecular surface information of both the complexes.

MEP represents the non-bonded interaction energy between ligands and receptors **[19]**. Hence, it was calculated for both the complexes to compare their ligand docking regions. The ligand docking region cleft (encircled with an arrow) of KN-MurF1-6MT is completely engulfed by a positive charge whereas in case of KN-MurF1-CP the ligand docking region is only partially engulfed by a positive charge **(Figure 5a & 5b)**. Thus, there is clear evidence of differences in their charge complementarity indicating tighter binding in KN-MurF1-CP than in KN-MurF1-6MT. Thus, MEPS analysis revealed basic differences in the ligand binding pocket, which could be

exploited in future for the rational design of selective KN-MurF bactericidals.
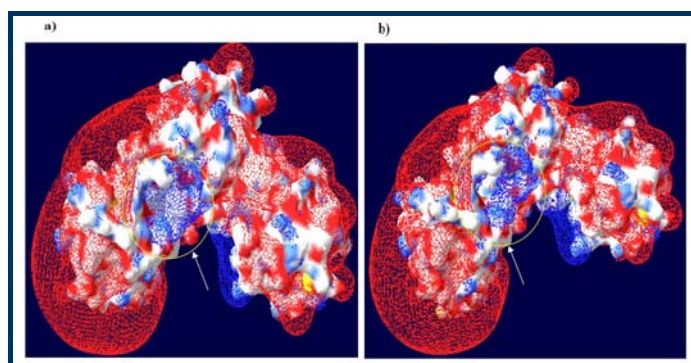

Figure 5: Molecular surface representation of KN-MurF1-6-MT Complex **(5a)** and KN-MurF1-CP Complex **(5b)** and their respective MEP represented as blue mesh (positive potential) and red mesh (negative potential). The encircled region represents their corresponding active site region.

Conclusion:

The KN-MurF homology model generated for the first time a 3D structural model that can be used for screening different molecules for KN-specific MurF inhibitory activity. The developed model showed good overall structural quality and was confirmed using several different validation tools. Our study provided structural insight about the hotspots HIS 281 and ASN 282 and their corresponding plausible potential charge interactions with ligands. Thus, the present work forms the basis for further molecular modeling and biochemical studies on targeting the KN-MurF enzyme for therapy. Our studies conclusively revealed 6-MT as a potent lead compound better than other ligands based on best values of docking energy, Ki value and HB interactions. Further, pre-clinical analysis of 6-MT is necessary to accurately understand its molecular mechanism of action and pharmacological efficiency to conclusively state it as an anti-bacterial analogue.

References:

[1] Moellering RC, *N Engl J Med*, 2010 **363**: 2377 [PMID: 21158655].
[2] Mohamudha PR *et al*. *Indian J Med Res*. 2012 135(1):114 [PMID: 22382192].
[3] Sidjabat H *et al*. *Clin Infect Dis*. 2011 **52**: 481 [PMID: 21258100].
[4] Bugg TD *et al*. *Trends Biotechnol*. 2011 **29:** 167 [PMID: 21232809].
[5] Turk S *et al*. *Bioorg Med Chem*. 2009 **17:** 1884 PMID: [19223185].
[6] Ma X *et al*. *J Ethnopharmacol*. 2011 **138**: 314 [PMID: 22004895].
[7] Cosconati S *et al*. *Expert Opin Drug Discov*. 2010 **5**: 597 [PMID: 21532931].
[8] Laoui A & Polyakov VR. *J Comput Chem*. 2011 **32**: 1944 [PMID: 21455963].
[9] Guex N & Peitsch MC, *Electrophoresis*. 1997 **18:** 2714 [PMID: 9504803].
[10] Pettersen EF *et al*. *J Comput Chem*. 2004 **25**: 1605 [PMID: 15264254].
[11] Adamczak R *et al*. *Proteins*. 2005 **59**: 467 [PMID: 15768403].
[12] Corpet F, *Nucl. Acids Res*. 1988 **16**: 10881 [PMID: 2849754].
[13] Gouet P *et al*. *Bioinformatics*. 1999 **15**: 305 [PMID: 10320398].
[14] Roy A, *Nature Protocols*. 2010 **5**: 725 [PMID: 20360707].
[15] Eisenberg D, *Methods in enzymology*. 1997 **277:** 396 [PMID: 9379925].
[16] Wiederstein M & Sippl MJ, *Nucl Acids Res*. 2007 **35:** 407 [PMID: 17517781].
[17] Nayeem A *et al*. *Protein Sci*. 2006 **15:** 808 [PMID: 16600997].
[18] Yan Y *et al*. *J Mol Biol*. 2000. **304**: 435 [PMID: 11090285].
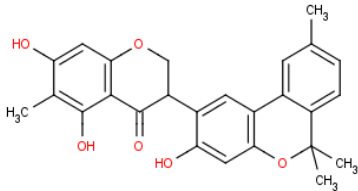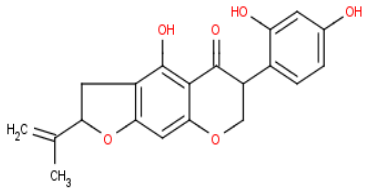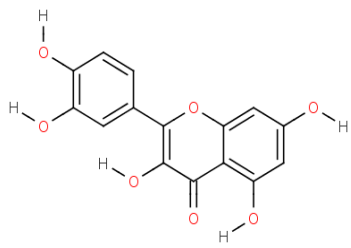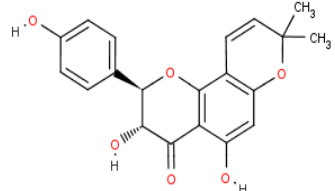[19] Kumar V *et al*. *J Mol Model*. 2011 **17**: 939 [PMID: 20614148]
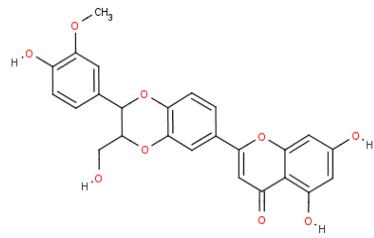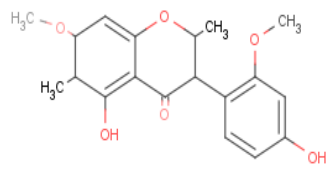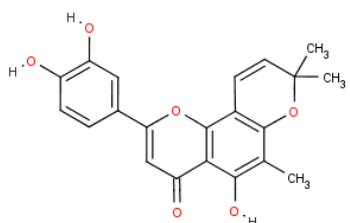
BIOINFORMATION

Supplementary martial:

Table 1: Lipinski values/ADME-Tox of *Desmodium* sp. phyto-ligands and Ciprofloxacin along with their structural representations

S. No	Compounds	Structures	Donor HB	Accpt HB	Mol MW	QPlog Po/w
1	6-Methyltetrapterol A		4	9.25	452.63	2.89
2	Uncinanone B		5	10.2	372.501	1.043
3	Quercetin		5	7	302.23	1.683
4	Yukovanol		4	9.25	370.485	1.434
5	Hydnocarpin		5	15.3	486.601	0.469
6	Uncinanone E		2	4.75	436.504	4.395
7	Desmodol		4	9.25	384.512	1.625
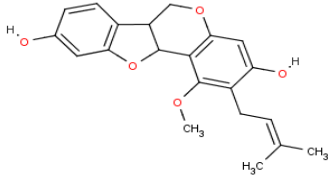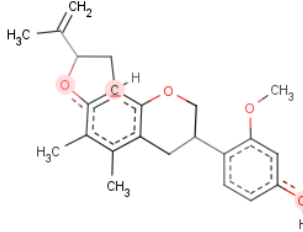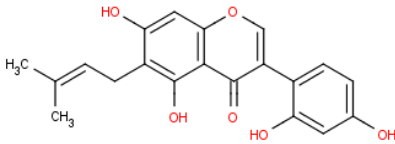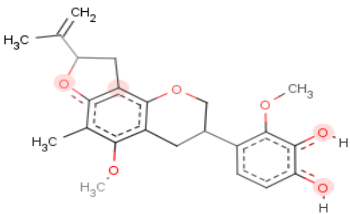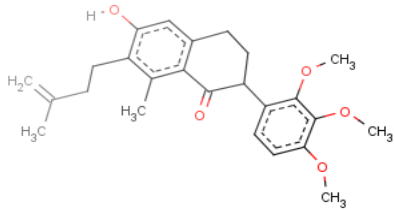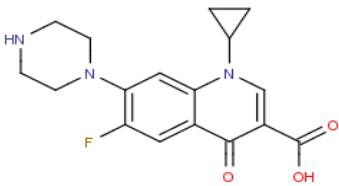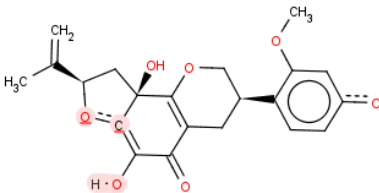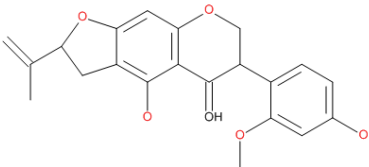
8	Edudiol		2	8.5	368.512	2.563
9	Desmodian C		1	6.8	380.567	4.232
10	Uncinanone A		5	10.2	372.501	1.043
11	Hydroxydesmodian B		2	10.2	412.565	2.84
12	Uncinanone D		2	8.5	426.635	3.985
13	Ciprofloxacin		1	6	331.346	0.28
14	Desmodian D		4	10.95	400.511	1.355
15	Uncinanone C		4	9.2	383.411	3.202

Table 2: Docking studies of *Desmodium* plant species derivatives with modelled MurF compared against Ciprofloxacin-MurF complex.

S.NO	COMPOUNDS	ΔG (KCAL MOL⁻¹)	INHIBITORY CONSTANT K_i (µM)	H-BOND INTERACTION	DISTANCE (Å)
1	6-Methyltetrapterol A	-8.7	1.22	PRO 278 O-H...O	2.140
				HIS 281 N-H...O	2.048
				ASN 282 O-H...O	3.711
2	Quercetin	-7.85	1.76	THR428 O-H...O	1.668
				THR260 O-H...O	1.697
				GLU349 O-H...O	1.81
3	Yukovanol	-7.84	1.79	ALA312 N-H...O	1.927
				PRO276 O-H...O	1.771
4	Uncinanone E	-7.72	5.03	VAL313 N-H...O	2.197
				ARG316 N-H...O	1.993
5	Desmodol	-7.56	2.89	ASN334 O-H...O	2.077
				ASN334O-H...O	1.853
6	Uncinanone C	-7.0	7.35	ARG316 O-H...O	2.065
7	Edudiol	-6.93	8.28	HIS281 N-H...O	1.901
				PRO278 O-H...O	1.877
				ARG316 N-H...O	2.223
8	DesmodianC	-6.74	11.42	SER325 N-H..O	1.93
9	Ciprofloxacin	-6.2	28.76	GLU116 O-H...O	1.892
				HIS 281 N-H...O	3.371
10	Uncinanone D	-5.93	45.04	HIS281 N-H...O	2.041